International Journal of Biochemistry and Cell Biology 110 (2019) 84–90

Contents lists available at ScienceDirect

International Journal of Biochemistry and Cell Biology

journal homepage: www.elsevier.com/locate/biocel

Loss of human arylamine *N*-acetyltransferase I regulates mitochondrial function by inhibition of the pyruvate dehydrogenase complex

Lili Wang, Rodney F. Minchin*, Patricia J. Essebier, Neville J. Butcher

Molecular and Cellular Pharmacology Laboratory, School of Biomedical Sciences, The University of Queensland, St Lucia, Brisbane, 4072 Australia

ARTICLE INFO

Keywords:
Arylamine *N*-acetyltransferase
Pyruvate dehydrogenase
Mitochondria

ABSTRACT

Human arylamine *N*-acetyltransferase 1 (NAT1) has been widely reported to affect cancer cell growth and survival and recent studies suggest it may alter cell metabolism. In this study, the effects of NAT1 deletion on mitochondrial function was examined in 2 human cell lines, breast carcinoma MDA-MB-231 and colon carcinoma HT-29 cells. Using a Seahorse XFe96 Flux Analyzer, NAT1 deletion was shown to decrease oxidative phosphorylation with a significant loss in respiratory reserve capacity in both cell lines. There also was a decrease in glycolysis without a change in glucose uptake. The changes in mitochondrial function was due to a decrease in pyruvate dehydrogenase activity, which could be reversed with the pyruvate dehydrogenase kinase inhibitor dichloroacetate. In the MDA-MB-231 and HT-29 cells, pyruvate dehydrogenase activity was attenuated either by an increase in phosphorylation or a decrease in total protein expression. These results may help explain some of the cellular events that have been reported recently in cell and animal models of NAT1 deficiency.

1. Introduction

Arylamine *N*-acetyltransferase 1 (NAT1, EC 2.3.1.5) is a cytosolic enzyme that catalyses the acetylation of small molecule arylamines, hydrazines and sulphonamides (Hein, 2002). Found in most cells in the body, NAT1 expression is regulated at the transcriptional and post-transcriptional levels (Butcher et al., 2007, 2008). A detailed evolutionary study of mammalian arylamine *N*-acetyltransferase s supports the notion that NAT1 has evolved through strong negative selection to conserve functionality over time (Sabbagh et al., 2013). This observation, along with its wide distribution in the body, suggests NAT1 has a role in addition to xenobiotic metabolism. The only known endogenous substrate for NAT1 is the folate catabolite *p*-aminobenzoylglutamate, but the physiological importance of *p*-aminobenzoylglutamate acetylation *in vivo* has been questioned (Witham et al., 2013). There is emerging evidence that NAT1 expression is associated with changes in cell growth and survival, cell morphology, and various intracellular metabolic pathways (Carlisle et al., 2016; Stepp et al., 2018; Tiang et al., 2011, 2010, 2015; Witham et al., 2013, 2017).

In addition to NAT1, humans express a second arylamine *N*-acetyltransferase (NAT2), the result of a gene duplication on chromosome 8. NAT2 levels are highest in the liver and gastrointestinal tract where it is important in the metabolism of drugs and other xenobiotics (Hein, 2002). Recently, single nucleotide polymorphisms in the NAT2 gene, which result in a slow acetylator phenotype, were shown to be associated with insulin resistance (Knowles et al., 2015). Moreover, deletion of the murine homolog of human NAT2 (Nat1) recapitulated the insulin resistance phenotype (Camporez et al., 2017), increased mitochondrial dysfunction and the production of reactive oxygen species (ROS) (Chennamsetty et al., 2016). Nat1 knockdown in 3T3-L1 cells with shRNA decreased both basal respiration as well as reserve respiratory capacity. A similar finding was reported for hepatocytes isolated from Nat1 null mice (Camporez et al., 2017), suggesting that human NAT2 (or mouse Nat1) is important for mitochondrial function. Previously, we reported that deletion of NAT1 in various human cells including MDA-MB-231 cells, using CRISPR/Cas9 technology decreased oxidative phosphorylation (Lichter et al., 2017). Moreover, in human HT-29 cells, glucose utilisation decreased and ROS production increased following NAT1 deletion (Wang et al., 2018). These studies suggested that NAT1 affected mitochondrial function in a similar manner to that seen following Nat1 knockdown in mice. However, a recent study using human breast MDA-MB-231 cells reported that deletion of NAT1 increased reserve respiratory capacity and glycolytic reserve (Carlisle et al., 2018). To better understand the effects of NAT1 on cell metabolism,

Abbreviations: NAT1, arylamine *N*-acetyltransferase 1; NAT2, arylamine *N*-acetyltransferase 2; AcCoA, acetylcoenzyme A; ROS, reactive oxygen species; OCR, oxygen consumption rate; ECAR, extracellular acidification rate; 2-NBDG, 2-*N*-7-nitrobenz-2-oxa-13-diazol-4-yl)amino)-2-deoxyglucose; GFP, green fluorescent protein gene; PDH, E1αPyruvate dehydrogenase-E1α; PDHK, pyruvate dehydrogenase kinase; DCA, dichloroacetate

* Corresponding author.
E-mail address: r.minchin@uq.edu.au (R.F. Minchin).

https://doi.org/10.1016/j.biocel.2019.03.002
Received 9 January 2019; Received in revised form 27 February 2019; Accepted 1 March 2019
Available online 02 March 2019

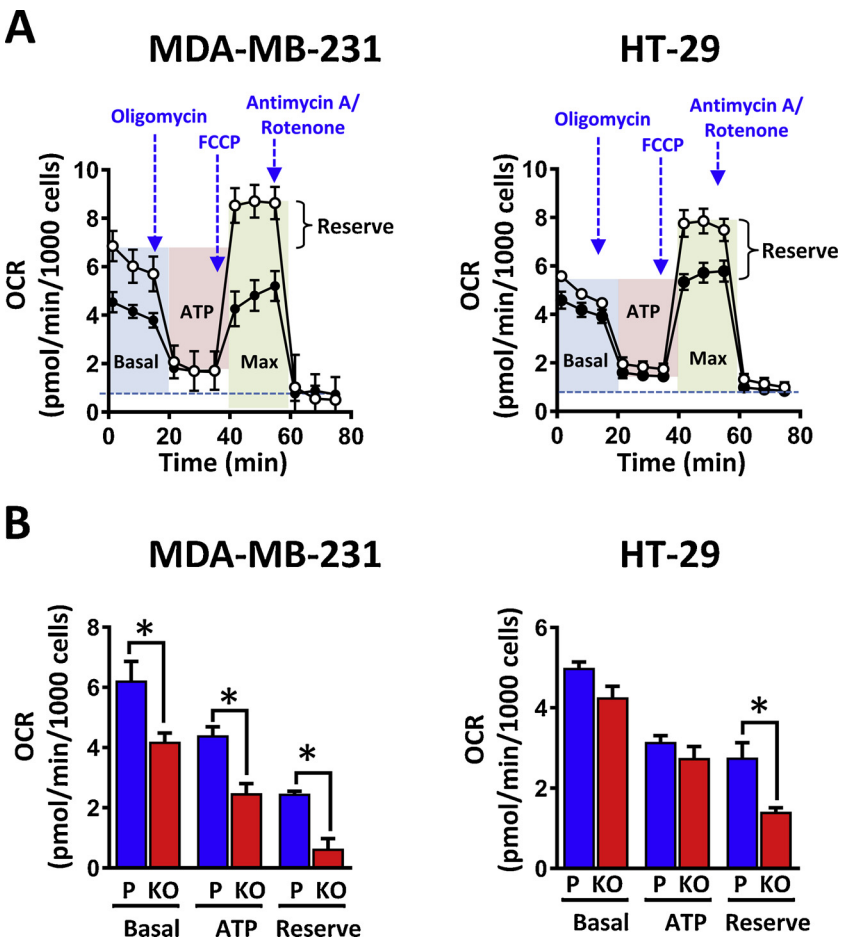

Fig. 1. NAT1 deletion decreases oxidative phosphorylation. (A) Oxygen consumption rates (OCR) were measured in parental (open symbols) or NAT1 deleted (closed symbols) MDA-MB-231 and HT-29 cells. Basal oxygen consumption (Basal), ATP-dependent respiration (ATP), maximum respiratory capacity (Max) and reserve respiratory capacity (Reserve) are shown on each graph. (B) Quantification of the different oxidative phosphorylation parameters in MDA-MB-231 and HT-29 parental (P) and NAT1 deleted (KO) cells. All data are the mean ± SEM (n = 4) normalized to cell number. Asterisks indicate significant differences by one-way ANOVA ($p < 0.05$).

glucose-mediated oxygen consumption and glycolysis were compared in 2 independent cell models following deletion of the NAT1 gene. The results show mitochondrial changes that may explain the link between arylamine *N*-acetyltransferase *N*-acetyltransferase expression and mitochondrial function.

2. Materials and methods

2.1. Cell lines and tissue culture

Human cancer cell lines MDA-MB-231 (breast adenocarcinoma) and HT-29 (colon adenocarcinoma) were obtained from the American Type Culture Collection (ATCC, Manassas, VA) and cultured in RPMI 1640 medium (Thermo Fisher Scientific, Carlsbad, CA) supplemented with 10% fetal bovine serum (Hyclone; *in vitro* Technologies, VIC, Australia), 100 units/ml penicillin/streptomycin and 2 mM L-glutamine in a humidified 5% CO_2 atmosphere at 37 °C. The HT-29 CRISPR/Cas9 NAT1 knockout cell line has been described previously (Wang et al., 2018). The MDA-MB-231 NAT1 knockout cell line was generated by disrupting the NAT1 gene using a human NAT1 gene knockout CRISPR/Cas9 kit (Origene Technologies, Rockville, MD; KN221042). NAT1 knockout was verified by PCR of genomic DNA, lack of NAT1 acetylation activity and Western blot for NAT1 protein, as previously described (Wang et al., 2018).

2.2. Mitochondrial bioenergetics

Basal oxygen consumption rate (OCR) and extracellular acidification rate (ECAR) were measured using a Seahorse XFe96 Flux Analyzer (Seahorse Bioscience, Billerica, MA) as described in the manufacturer's instructions. Cells were seeded at 2×10^4 cells per well in 96-well plates and a sensor cartridge was hydrated in Seahorse XF Calibrant (Seahorse Bioscience) at 37 °C in a non−CO_2 incubator on the day prior to assay. On the day of assay, the growth medium was changed to Seahorse XF assay medium (Seahorse Bioscience; pH 7.4) and the plate was incubated for 1 h at 37 °C in a non−CO_2 incubator. Basal OCR was first measured, followed by sequential injections of oligomycin (1 μM), carbonyl cyanide 4-trifluoromethoxy-phenylhydrazone (FCCP; 0.5 μM) and antimycin A/rotenone (1 μM). ECAR was measured following sequential injections of glucose (10 mM), oligomycin (1 μM) and 2-deoxy-D-glucose (50 mM). Measurements were standardized to cell number in each well.

2.3. Glucose uptake assay

Glucose uptake was quantified using 2-(N-(7-nitrobenz-2-oxa-1,3-diazol-4-yl)amino)-2-deoxyglucose (2-NBDG; Cayman Chemical Company, Ann Arbor, MI), a fluorescent-labelled glucose analog. Briefly, cells were seeded in 96-well plates at 5×10^3 cells/well and allowed to adhere overnight. The medium was then changed to 100 μl glucose-free medium containing 10 μM 2-NBDG for 1 h at 37 °C. After washing three times with ice-cold phosphate buffered saline (PBS), cells were lysed with 100 μl Passive Lysis Buffer (Promega, Madison, WI) for 10 min at room temperature. The fluorescence of 2-NBDG was measured using a microplate reader (E x 485 nm, Em 535 nm) and normalized to total protein.

2.4. Western blotting

Parent and NAT1 KO cells were seeded in 6-well plates at 6×10^5

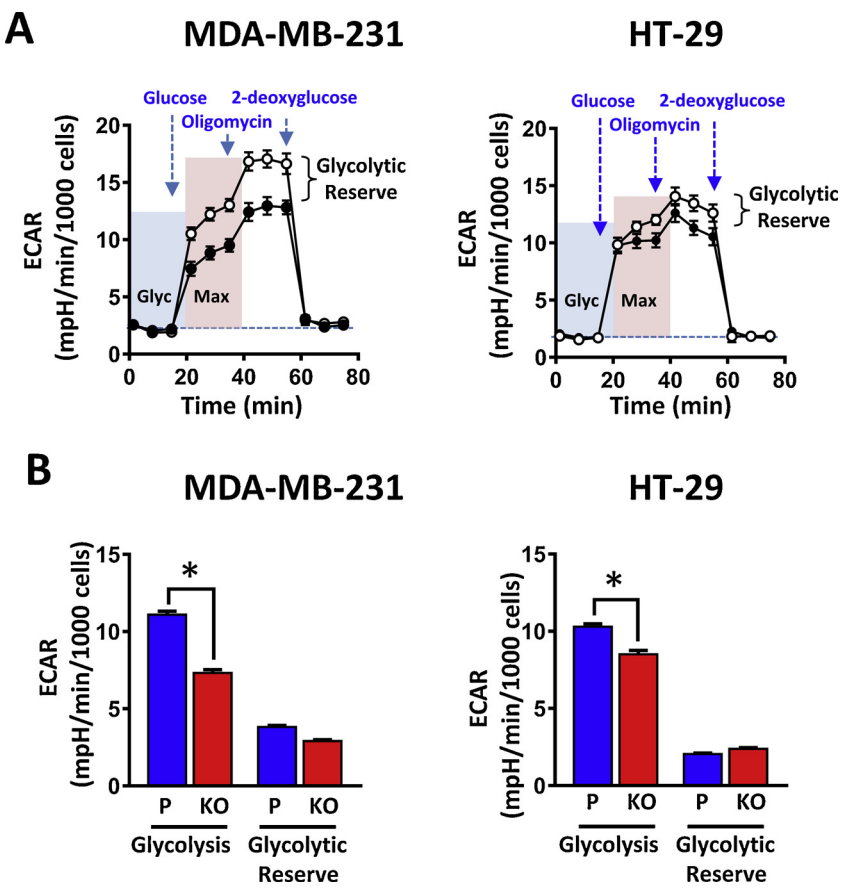

Fig. 2. NAT1 deletion decreases glycolysis. (A) Extracellular acidification rates (ECAR) were measured in parental (open symbols) or NAT1 deleted (closed symbols) MDA-MB-231 and HT-29 cells. Glycolysis (Glyc), maximum glycolytic capacity (Max) and glycolytic reserve are shown on each graph. (B) Quantification of the different glycolysis parameters in MDA-MB-231 and HT-29 parental (P) and NAT1 deleted (KO) cells. All data are the mean ± SEM (n = 4) normalized to cell number. Asterisks indicate significant differences by one-way ANOVA ($p < 0.05$).

cells/well and cultured for 48 h. Some cells were treated with 10 mM DCA for the final 24 h of culture. Cells were then washed twice with ice-cold PBS and lysed directly in 1× Laemmli buffer containing protease and phosphatase inhibitor cocktail (Sigma-Aldrich). Proteins were separated by SDS-PAGE and transferred to nitrocellulose membranes. The blots were blocked with 5% bovine serum albumin in Tris-buffered saline overnight at 4 °C with rocking. Blots were then incubated with anti-pyruvate dehydrogenase E1-alpha subunit antibody (Abcam, Cambridge, UK; ab110330, 1:1000), anti-pyruvate dehydrogenase E1-alpha subunit (phospho S293) antibody (Abcam, ab177461, 1:1000) and anti-alpha-tubulin antibody (Cell Signaling Technology, Danvers, MA; #3873, 1:2000) diluted in blocking buffer overnight at 4 °C, followed by horseradish peroxidase-conjugated secondary antibodies (Jackson ImmunoResearch Laboratories, West Grove, PA) for 1 h at room temperature. Detection was by ECL using Westar ETA C2.0 substrate (Cyanagen, Bologna, Italy) and a Kodak Image Station 4000 s pro.

2.5. Pyruvate dehydrogenase assay

MDA-MB-231 and HT-29 cells were plated at a density of 0.6×10^6 cells per well in 6-well plates. After 24 h, the cells were washed twice with ice-cold PBS and scraped into PBS containing protease and phosphatase inhibitors cocktails (Sigma-Aldrich). The cells were then disrupted on ice using a Branson Sonifier 250 (2 × 5 s bursts, output = 4) and centrifuged at 1500 × *g* for 5 min at 4 °C. Supernatants were assayed for. pyruvate dehydrogenase according to the method of Ke et al (Ke et al., 2014). Briefly, 40 µL of cell supernatant was incubated with 1 mM $MgCl_2$, 0.2 mM thiamine pyrophosphate, 0.5 mM 3-(4,5-dimethylthiazol-2-yl)-2,5-diphenyltetrazolium bromide, 6.5 mM phenazine methosulfate and 2 mM sodium pyruvate in PBS. The reaction was run for 3 h at 37 °C following which absorbance was measured at 266 nm. An extinction coefficient of 18.65 $mM^{-1} cm^{-1}$ was used to calculate enzyme activity.

2.6. Data analysis

Data are presented as mean ± SEM. Statistical significance was determined by one-way ANOVA with p-values of 0.05 or less considered significant (GraphPad Software, San Diego, CA). Western blots were quantified by densitometry using ImageJ software.

3. Results

NAT1 deletion in MDA-MB-231 and HT-29 cells was confirmed by the lack of enzyme activity and the absence of NAT1 mRNA in the knockout cells. Sequencing was used to confirm insertion of the GFP gene in both NAT1 alleles in the MDA-MD-231 cells and the single NAT1 allele in the HT-29 cells (these cells carry a large deletion in one copy of 8p22).

To determine the effect of NAT1 deletion on mitochondrial function, OCR and ECAR were measured using a Seahorse XFe96 Flux Analyzer. In MDA-MB-231 cells, basal oxygen consumption, ATP-coupled oxygen consumption and reserve respiratory capacity decreased in the NAT1 knockout cells compared to parental cells (Fig. 1A & B, left panels). These results are consistent with a decrease in glucose flux through the mitochondria following NAT1 deletion. In the HT-29 cells, OCR was also decreased with the largest, and most significant, change seen in the reserve respiratory capacity (Fig. 1A & B, right panels).

In addition to oxidative phosphorylation, ATP requirements can be met by aerobic glycolysis where glucose is diverted to lactic acid instead of entering the TCA cycle. This is common in cells with mitochondrial dysfunction. Glycolysis was measured in each cell line by quantification of ECAR following the addition of glucose. In both MDA-MB-231 and HT-29 cells, glycolysis significantly decreased following

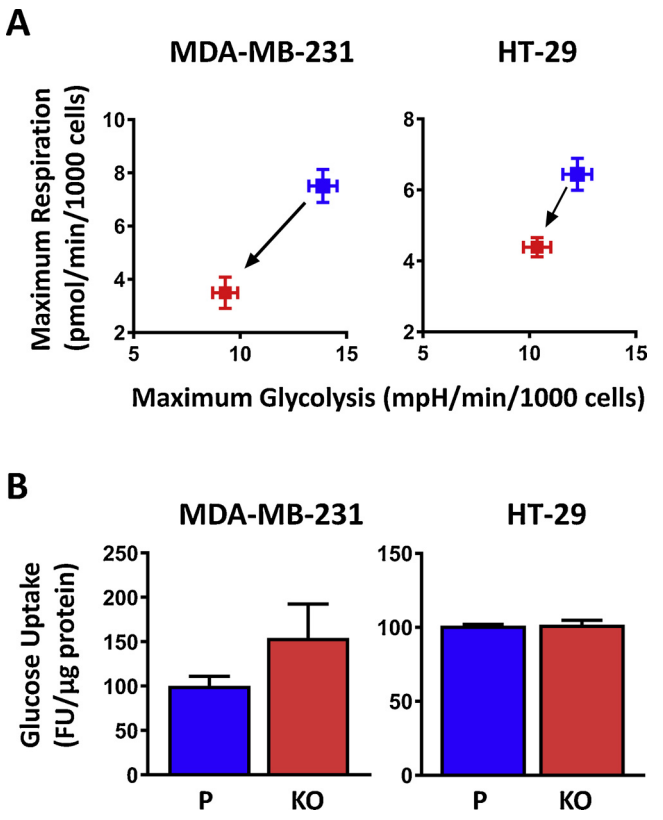

Fig. 3. (A) Bioenergetics plot for parental (blue symbols) and NAT1 deleted (red symbols) cells. (B) Effect of NAT1 deletion on glucose uptake measured using 2-(N-(7-nitrobenz-2-oxa-1,3-diazol-4-yl)amino)-2-deoxyglucose (2-NBDG). Results are expressed as fluorescent units normalized to total cellular protein. All data are the mean ± SEM (n = 5) (For interpretation of the references to colour in this figure legend, the reader is referred to the web version of this article).

NAT1 deletion (Fig. 2A & B). However, no change was seen with the glycolytic reserve.

To compare glucose metabolism *via* oxidative phosphorylation to that *via* glycolysis, a bioenergetics plot was constructed (Fig. 3A). In most cells, a decrease in one bioenergetics pathway is compensated by an increase in the other. However, following NAT1 deletion, there was a decrease in both oxidative phosphorylation and glycolysis indicating a shifted to a lower overall bioenergetic state. These results suggest that NAT1 knockout cells do not utilize glucose for glycolysis or oxidative phosphorylation to the same extent as the parental cells. To determine whether this difference was due to a decrease in glucose uptake, the accumulation of the glucose transporter probe 2-NBDG was measured. However, there was no significant difference in glucose transport in either cell line following NAT1 deletion (Fig. 3B). Taken together, these results suggest that glucose flux in the knockout cells is diverted away from the glycolysis/oxidative phosphorylation pathway.

The reserve respiratory capacity is essential for cell survival during mitochondrial stress. It is partly dependent on activity of the mitochondrial pyruvate dehydrogenase complex and a loss in activity can reduce or eliminate reserve respiratory capacity (Pfleger et al., 2015; Prabhu et al., 2015). To determine whether deletion of NAT1 altered pyruvate dehydrogenase complex function, enzyme activity was measured in both parental and knockout MDA-MB-231 and HT-29 cells (Fig. 4A & B). For both cell lines, there was a significant decrease in activity following NAT1 deletion.

Pyruvate dehydrogenase-E1α (PDH-E1α) is an essential component of the pyruvate dehydrogenase complex and is regulated by reversible phosphorylation catalysed by pyruvate dehydrogenase kinase (PDHK). Phosphorylation of PDH-E1α results in a decrease in activity of the pyruvate dehydrogenase complex. When MDA-MB-231 and HT-29 knockout cells were treated with the PDHK inhibitor dichloroacetate (DCA), the changes seen in OCR were completely rescued (Fig. 4C & D) suggesting that NAT1 deletion may induce PDH-E1α phosphorylation. To test this, both total and phosphorylated PDH-E1α were quantified in parental and NAT1 knockout cells (Fig. 5A). For the MDA-MD-231 cells, there was a 3-fold increase in phosphorylated PDH-E1α following NAT1 knockout. DCA treatment of the NAT1 deleted cells reversed this increase to levels seen in the parental cells (Fig. 5B). By contrast, total PDH-E1α decreased in the HT-29 NAT1 knockout cells. When these cells were treated with DCA, PDH-E1α increased to levels similar to the parental cells (Fig. 5C) showing that loss of PDH-E1α following NAT1 knockout was reversed by DCA treatment.

4. Discussion

When NAT1 was deleted from MDA-MB-231 and HT-29 cells, there was a marked decrease in oxidative phosphorylation, which was associated with a decrease in PDH-E1α activity. Inhibition of the pyruvate dehydrogenase complex limits pyruvate entry into the TCA cycle and lowers ATP generation. A common response in cancer cells to a change in oxidative phosphorylation is metabolically switching to aerobic glycolysis, which can maintain ATP production. However, this was not the case following NAT1 deletion in either cell line as glycolysis was also diminished. Since glucose uptake was not altered, these results suggest glucose was shunted away from the glycolytic/oxidative phosphorylation pathways towards other pathways such as glycogenesis, the pentose phosphate pathway or the hexosamine synthesis pathway (Hay, 2016). The mechanism for this remains to be determined. However, a recent metabolomics study using NAT1 deleted MDA-MB-231 cells identified changes in numerous polar metabolites, although most remain to be definitively identified (Carlisle et al., 2016). Nevertheless, that study demonstrated marked changes in metabolism following NAT1 deletion.

The changes in mitochondrial function in the MDA-MB-231 and HT-29 cells are similar to those reported in murine cells following Nat1 knockout (Camporez et al., 2017; Chennamsetty et al., 2016). Nat1 is the murine homolog of human NAT2, not NAT1, so the similarity in responses following gene deletion was unexpected. These observations suggest that NAT1 and NAT2 may have common or redundant biological roles in regulating mitochondrial function. Alternatively, since NAT1 and NAT2 are differentially expressed *in vivo*, they may have similar roles but in different tissues in the body. Interestingly, when we quantified NAT2 expression in the MDA-MD-231 and HT-29 cells by qPCR following NAT1 knockout, there was a 3.5 ± 0.6 and 2.0 ± 0.5 fold increase in mRNA compared to the parental cells, respectively ($p < 0.01$). This suggests that expression of NAT1 and NAT2 are not completely independent, an observation supported by a positive association between the expression of the 2 genes in human breast cancer cells (Carlisle and Hein, 2018).

The effect of NAT1 deletion on mitochondrial function in MDA-MB-231 cells has been reported elsewhere (Carlisle et al., 2018). However, unlike the data presented here, increases in reserve capacity and glycolytic reserve were seen. The reasons for this variance between our study and that of Carlisle et al studies is not immediately obvious. There were differences in the gene deletion protocols that may have contributed to varying phenotypes. There may also be important differences associated with how the gene-deleted cells were selected and cultured. It will be important in the future to identify the molecular mechanisms for the difference in mitochondrial function reported here and by Carlisle et al (Carlisle et al., 2018).

In HT-29 cells, mitochondrial function also decreased following NAT1 deletion due to an attenuated PDH activity. However, the mechanism involved a decrease in total PDH protein, not an increase in phosphorylation as seen in the MDA-MB-231 cells. While there is much known about the regulation of PDH by PDHKs, very little is known

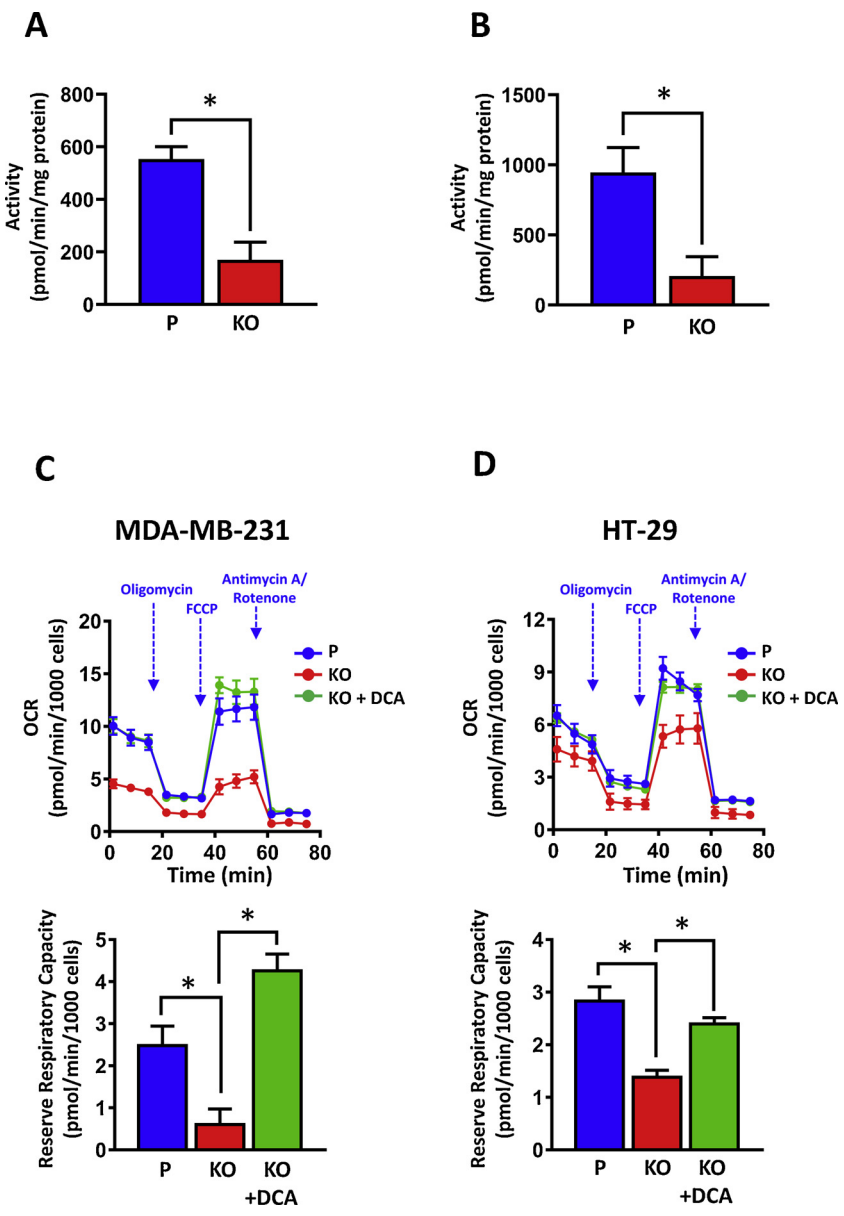

Fig. 4. Effect of NAT1 deletion on pyruvate dehydrogenase complex. (A) Enzyme activity of the pyruvate dehydrogenase complex in parental (P) and knockout (KO) MDA-MD-231 cells. (B) Enzyme activity of the pyruvate dehydrogenase complex in parental and knockout HT-29 cells. (C and D) Effect of DCA on oxidative phosphorylation in MDA-MB-231 (C) and HT-29 (D) cells. The upper graphs show OCR in parental cells, NAT1 knockout cells and NAT1 knockout cells treated with 10 mM dichloroacetate (KO + DCA). The lower graphs show quantification of reserve respiratory capacity for each of the cell lines. Data are the mean ± SEM (n = 4). Asterisks indicate significant differences by one-way ANOVA ($p < 0.05$).

about its stability. PDH is down-regulated in rat liver following treatment with β-hydroxybutyrate (Sharma et al., 2005) and during the development of dilated cardiomyopathy (Missihoun et al., 2009). Importantly, the protein is stabilized by DCA, both *in vitro* and *in vivo*. This was also seen in the present study (Fig. 5C) and explains why DCA was able to rescue the changes in mitochondrial function following NAT1 deletion.

Regardless of whether PDH activity was down-regulated by phosphorylation or by loss of total PDH protein, the metabolic outcomes were similar suggesting that the effect of NAT1 deletion was to decrease metabolic capacity. Many functional changes observed following NAT1 inhibition are cell-type dependent. For example, in HT-29 cells (Tiang et al., 2011) and MDA-MB-231 cells (Stepp et al., 2018), low NAT1 activity was associated with slower growth and inhibition of colony formation in soft agar. This is consistent with a lower metabolic capacity. By contrast, no changes were observed in HeLa cells (Witham et al., 2017). In MDA-MB-231 and MDA-MB-436 cells, knockdown of NAT1 with shRNA induced morphological changes and decreased invasiveness. However, this was not seen in BT-549 cells (Tiang et al., 2015). Deletion of the NAT1 gene increased reactive oxygen (ROS) production and apoptosis, especially under nutrient stress, in HT-29 cells but not in HeLa cells (Wang et al., 2018).

The current study has identified diminished PDH activity as central to the changes in mitochondrial function following NAT1 deletion, a least in MDA-MB-231 and HT-29 cells. These results may help explain some of the cellular changes that have been reported recently in cell and animal models of NAT1 and NAT2 deficiency. For NAT2, there is a strong insulin resistance phenotype reported in humans carrying the slow acetylator allele (rs1208 “A”) (Knowles et al., 2015). It will be important to determine whether these individuals have altered PDH activity in peripheral tissues. If so, genotyping diabetic patients for NAT1 /or NAT2 polymorphisms may identify a patient sub-population that could benefit from treatment with PDH activators, such as DCA

Author contributions

The project was conceptualized and designed by RFM and NJB. LW, RFM, PE and NJB performed the experiments and analysed the data. RFM wrote the manuscript, which was read and edited by all authors.

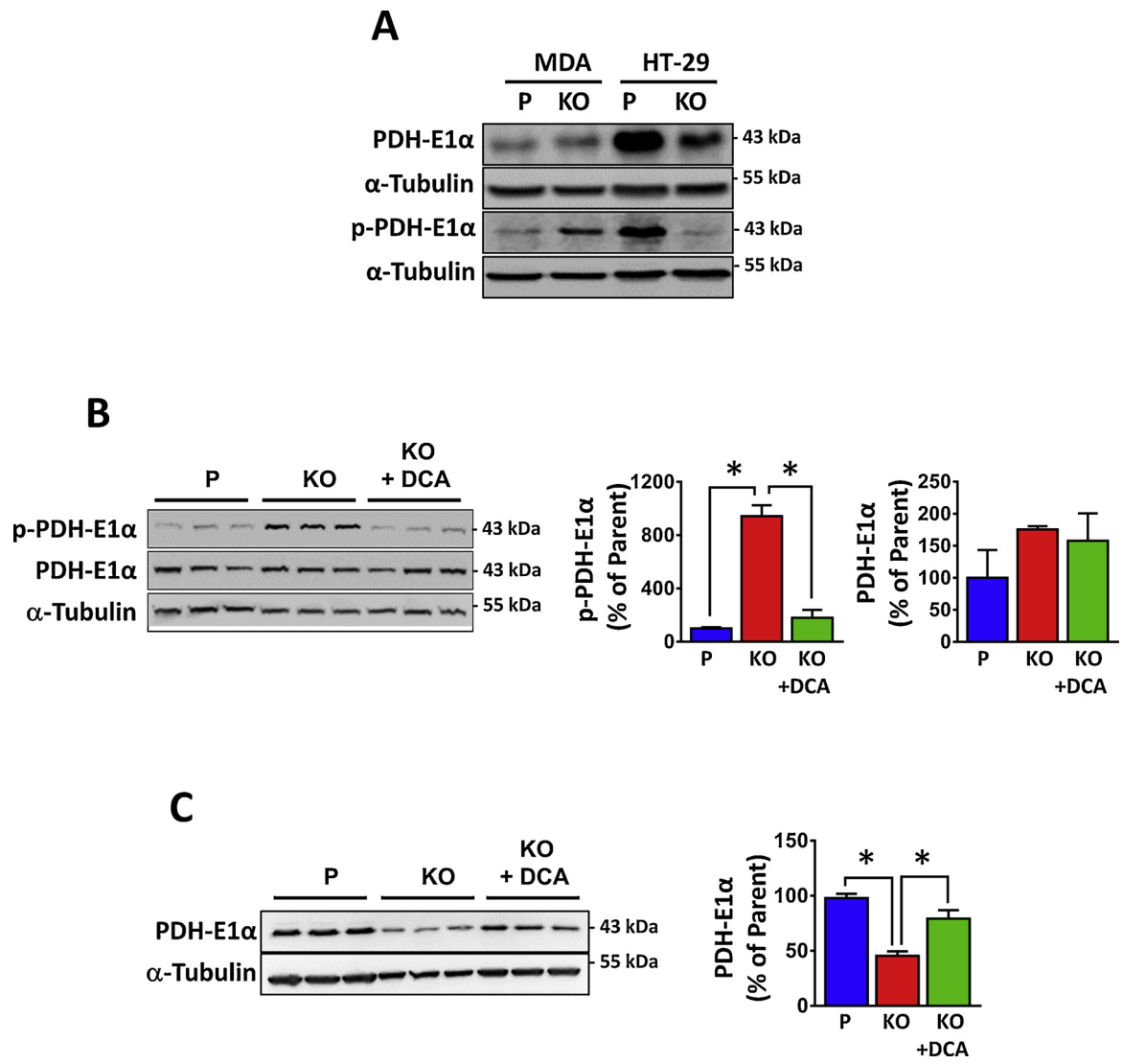

Fig. 5. Effect of NAT1 deletion on pyruvate dehydrogenase expression. (A) Expression of PDH-E1α and phosphorylated PDH-E1α (p-PDH-E1α) in parental (P) and NAT1 knockout (KO) cells is shown for both MDA-MB-231 (MDA) and HT-29 cells. (B) The effect of 10 mM DCA on p-PDH-E1α levels in MDA-MB-231 cells. Quantification of the proteins relative to α-tubulin is shown to the right. (C) The effect of 10 mM DCA on PDH-E1α levels in HT-29 cells. Quantification of the proteins relative to α-tubulin is shown to the right. All data are the mean ± SEM (n = 3). Asterisks indicate significant differences by one-way ANOVA ($p < 0.05$).

Conflict of interest

The authors declare no potential conflict of interest.

Acknowledgement

This work was supported by the National Health and Medical Research Council of Australia (Grant # 1024769)

References

Butcher, N.J., Tetlow, N.L., Cheung, C., Broadhurst, G.M., Minchin, R.F., 2007. Induction of human arylamine N-acetyltransferase type I by androgens in human prostate cancer cells. Cancer Res. 67 (1), 85–92.

Butcher, N.J., Tiang, J., Minchin, R.F., 2008. Regulation of arylamine N-acetyl-transferases. Curr. Drug Metab. 9 (6), 498–504.

Camporez, J.P., Wang, Y., Faarkrog, K., Chukijrungroat, N., Petersen, K.F., Shulman, G.I., 2017. Mechanism by which arylamine N-acetyltransferase 1 ablation causes insulin resistance in mice. Proc. Natl. Acad. Sci. U. S. A. 114 (52) E11285-e11292.

Carlisle, S.M., Hein, D.W., 2018. Retrospective analysis of estrogen receptor 1 and Nacetyltransferase gene expression in normal breast tissue, primary breast tumors, and established breast cancer cell lines. Int. J. Oncol. 53 (2), 694–702.

Carlisle, S.M., Trainor, P.J., Yin, X., Doll, M.A., Stepp, M.W., States, J.C., Zhang, X., Hein, D.W., 2016. Untargeted polar metabolomics of transformed MDA-MB-231 breast cancer cells expressing varying levels of human arylamine N-acetyltransferase 1. Metabolomics 12 (7).

Carlisle, S.M., Trainor, P.J., Doll, M.A., Stepp, M.W., Klinge, C.M., Hein, D.W., 2018. Knockout of human arylamine N-acetyltransferase 1 (NAT1) in MDA-MB-231 breast cancer cells leads to increased reserve capacity, maximum mitochondrial capacity, and glycolytic reserve capacity. Mol. Carcinog.

Chennamsetty, I., Coronado, M., Contrepois, K., Keller, M.P., Carcamo-Orive, I., Sandin, J., Fajardo, G., Whittle, A.J., Fathzadeh, M., Snyder, M., Reaven, G., Attie, A.D., Bernstein, D., Quertermous, T., Knowles, J.W., 2016. Nat1 deficiency is associated with mitochondrial dysfunction and exercise intolerance in mice. Cell Rep. 17 (2), 527–540.

Hay, N., 2016. Reprogramming glucose metabolism in cancer: can it be exploited for cancer therapy? Nat. Rev. Cancer 16 (10), 635–649.

Hein, D.W., 2002. Molecular genetics and function of NAT1 and NAT2: role in aromatic amine metabolism and carcinogenesis. Mutat. Res. 506-507, 65–77.

Ke, C.-J., He, Y.-H., He, H.-W., Yang, X., Li, R., Yuan, J., 2014. A new spectrophotometric assay for measuring pyruvate dehydrogenase complex activity: a comparative evaluation. Anal. Methods 6 (16), 6381–6388.

Knowles, J.W., Xie, W., Zhang, Z., Chennemsetty, I., Assimes, T.L., Paananen, J., Hansson, O., Pankow, J., Goodarzi, M.O., Carcamo-Orive, I., Morris, A.P., Chen, Y.-D.I., Mäkinen, V.-P., Ganna, A., Mahajan, A., Guo, X., Abbasi, F., Greenawalt, D.M., Lum, P., Molony, C., Lind, L., Lindgren, C., Raffel, L.J., Tsao, P.S., Schadt, E.E., Rotter, J.I., Sinaiko, A., Reaven, G., Yang, X., Hsiung, C.A., Groop, L., Cordell, H.J., Laakso, M., Hao, K., Ingelsson, E., Frayling, T.M., Weedon, M.N., Walker, M., Quertermous, T., 2015. Identification and validation of N-acetyltransferase 2 as an insulin sensitivity gene. J. Clin. Invest. 125 (4), 1739–1751.

Lichter, J., Golka, K., Sim, E., Blomeke, B., 2017. Recent progress in N-acetyltransferase

research: 7th international workshop on N-acetyltransferases (NAT): workshop report. Arch. Toxicol. 91 (7), 2715–2718.
Missihoun, C., Zisa, D., Shabbir, A., Lin, H., Lee, T., 2009. Myocardial oxidative stress, osteogenic phenotype, and energy metabolism are differentially involved in the initiation and early progression of δ-sarcoglycan-null cardiomyopathy. Mol. Cell. Biochem. 321 (1-2), 45–52.
Pfleger, J., He, M., Abdellatif, M., 2015. Mitochondrial complex II is a source of the reserve respiratory capacity that is regulated by metabolic sensors and promotes cell survival. Cell Death Dis. 6, e1835.
Prabhu, A., Sarcar, B., Miller, C.R., Kim, S.H., Nakano, I., Forsyth, P., Chinnaiyan, P., 2015. Ras-mediated modulation of pyruvate dehydrogenase activity regulates mitochondrial reserve capacity and contributes to glioblastoma tumorigenesis. Neuro Oncol 17 (9), 1220–1230.
Sabbagh, A., Marin, J., Veyssière, C., Lecompte, E., Boukouvala, S., Poloni, E.S., Darlu, P., Crouau-Roy, B., 2013. Rapid birth-and-death evolution of the xenobiotic metabolizing NAT gene family in vertebrates with evidence of adaptive selection. BMC Evol. Biol. 13 62-62.
Sharma, P., Walsh, Kane T., Kerr-Knott, Kimberly A., Karaian, John E., Mongan, Paul D., 2005. Pyruvate modulates hepatic mitochondrial functions and reduces apoptosis indicators during hemorrhagic shock in rats. Anesthesiology 103 (1), 65–73.
Stepp, M.W., Doll, M.A., Carlisle, S.M., States, J.C., Hein, D.W., 2018. Genetic and small molecule inhibition of arylamine N-acetyltransferase 1 reduces anchorage-independent growth in human breast cancer cell line MDA-MB-231. Mol. Carcinog. 57 (4), 549–558.
Tiang, J.M., Butcher, N.J., Minchin, R.F., 2010. Small molecule inhibition of arylamine N-acetyltransferase Type I inhibits proliferation and invasiveness of MDA-MB-231 breast cancer cells. Biochem. Biophys. Res. Commun. 393 (1), 95–100.
Tiang, J.M., Butcher, N.J., Cullinane, C., Humbert, P.O., Minchin, R.F., 2011. RNAi-mediated knock-down of arylamine N-acetyltransferase-1 expression induces E-cadherin up-regulation and cell-cell contact growth inhibition. PLoS One 6 (2) e17031.
Tiang, J.M., Butcher, N.J., Minchin, R.F., 2015. Effects of human arylamine N-acetyltransferase I knockdown in triple-negative breast cancer cell lines. Cancer Med. 4 (4), 565–574.
Wang, L., Minchin, R.F., Butcher, N.J., 2018. Arylamine N-acetyltransferase 1 protects against reactive oxygen species during glucose starvation: Role in the regulation of p53 stability. PLoS One 13 (3) e0193560.
Witham, K.L., Butcher, N.J., Sugamori, K.S., Brenneman, D., Grant, D.M., Minchin, R.F., 2013. 5-methyl-tetrahydrofolate and the S-adenosylmethionine cycle in C57BL/6J mouse tissues: gender differences and effects of arylamine N-acetyltransferase-1 deletion. PLoS One 8 (10) e77923.
Witham, K.L., Minchin, R.F., Butcher, N.J., 2017. Role for human arylamine N-acetyltransferase 1 in the methionine salvage pathway. Biochem. Pharmacol. 125, 93–100.